

## Supplementary Materials for

### **Mate discrimination among subspecies through a conserved olfactory pathway**

Mohammed A. Khallaf, Thomas O. Auer, Veit Grabe, Ana Depetris-Chauvin, Byrappa Ammagarahalli, Dan-Dan Zhang, Sofia Lavista-Llanos, Filip Kaftan, Jerrit Weißflog, Luciano M. Matzkin, Stephanie M. Rollmann, Christer Löfstedt, Aleš Svatoš, Hany K. M. Dweck, Silke Sachse, Richard Benton, Bill S. Hansson\*, Markus Knaden\*

\*Corresponding author. Email: [mknaden@ice.mpg.de](mailto:mknaden@ice.mpg.de) (M.K.); [hansson@ice.mpg.de](mailto:hansson@ice.mpg.de) (B.S.H.)

Published 17 June 2020, *Sci. Adv.* **6**, eaba5279 (2020)

DOI: [10.1126/sciadv.aba5279](https://doi.org/10.1126/sciadv.aba5279)

#### **The PDF file includes:**

Figs. S1 to S7  
Table S1  
Legends for movies S1 to S9  
Legend for data file S1  
Text S1  
References

#### **Other Supplementary Material for this manuscript includes the following:**

(available at [advances.sciencemag.org/cgi/content/full/6/25/eaba5279/DC1](https://advances.sciencemag.org/cgi/content/full/6/25/eaba5279/DC1))

Movies S1 to S9  
Data file S1

**Fig. S1**

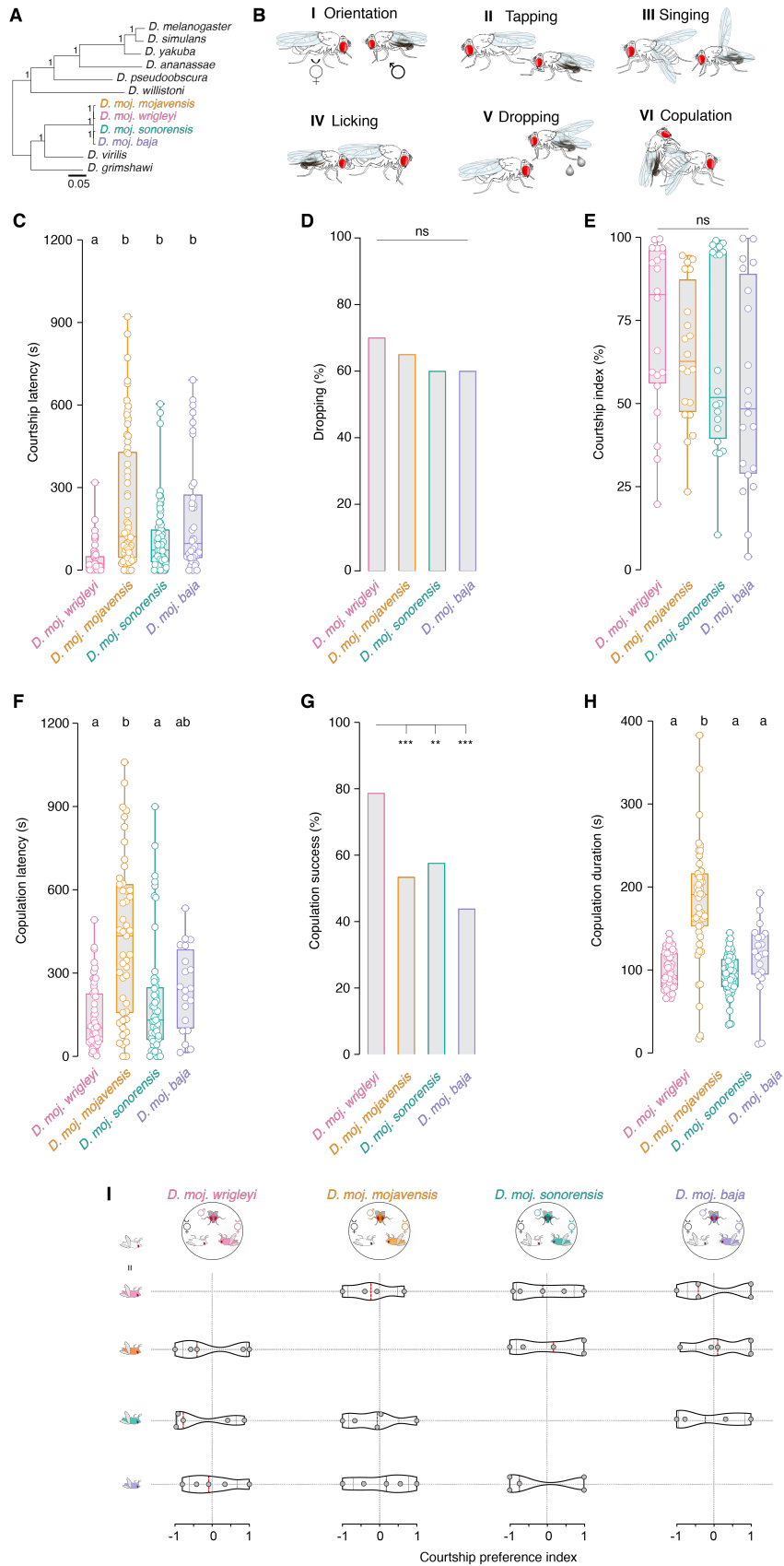


**Fig. S1. Sexual behaviors of *D. mojavensis* subspecies.**

**(A)** Phylogenetic relationship among the four *D. mojavensis* subspecies and other *Drosophila* species using the recent genomic analysis of *D. mojavensis* (22) and the *D. virilis*, *D. grimshawi*, *D. willistoni*, *D. pseudoobscura*, *D. ananassae*, *D. yakuba*, *D. simulans*, and *D. melanogaster* FlyBase assemblies

(FB2019\_04) based on concatenated sequences of 2177 loci. Scale bar for branch length represents the number of substitutions per site. Bootstrap values are indicated by the numbers at the nodes.

**(B)** Schematic drawing of courtship behaviors of the four *D. mojavensis* subspecies. **(I)** orientation, **(II)** tapping with forelegs, **(III)** singing by wing fanning, **(IV)** licking the female genitals, **(V)** anal droplet discharge, and **(VI)** copulation attempt. Fly drawings were adapted with permission from (58).

**(C)** Courtship latency of males toward virgin con-subspecific females in seconds (s) within a 20-minute time window. During the first minute, most males were eager to court by orienting and following the females. Among the four subspecies, *D. moj. wrigleyi* males exhibited shorter and less variable latencies to court. In this and the below panels, age of males and females is 10 days. Boxplots show the median, first and third quartile of the data. Different letters indicate significant differences between subspecies, Kruskal-Wallis test with Dunn's post-hoc correction ( $n$  from left to right = 60, 63, 74, and 38 replicates).

**(D)** Percentage of males that released a fluidic droplet from their anus while courting the female. This panel reveals that more than half of the tested males while courting the female released a fluidic droplet from their anus. See fig. S2G for chemical analysis of these droplets. Courtship behaviors were recorded by GoPro Camera (Watch movies S1 to S4 for details). Ns  $P > 0.05$ , Fisher's exact test ( $n = 10-20$  per subspecies).

**(E)** Courtship index [%] that males display toward their virgin con-subspecific females. In response to the rapid male courtship elements, females slow down their movement, quiver their abdomen, vibrate their wings, and scissor them as signs for acceptance, while kicking with legs or accelerating the movement speed to signal rejection (Watch movies S1 to S4). Overall, courtship rituals were comparable among the four subspecies. Ns  $P > 0.05$ , Kruskal-Wallis test with Dunn's post-hoc correction ( $n = 20$ ).

**(F)** Copulation latency in seconds (s). Males exhibiting no courtship behavior were excluded from analysis. *D. moj. wrigleyi* males exhibited shorter and less variable latencies to copulate. Kruskal-Wallis test with Dunn's post-hoc correction ( $n$  from left to right (the number of successful copulations in fig. S1B) = 52, 47, 53, and 20).

**(G)** Copulation success [%] of virgin couples in the different *D. mojavensis* subspecies within a 20-minute time window. Among the four subspecies, *D. moj. wrigleyi* males exhibited a higher percentage to be accepted for copulation. Fisher's exact test ( $n$  (from left to right) = 60, 63, 74, and 38 replicates).

**(H)** Copulation duration of *D. mojavensis* subspecies in seconds (s). Unlike the prolonged copulation time in *D. melanogaster* ( $\geq 15$  min) (59), copulation lasts for  $\sim 2-3$  min in the *D. mojavensis* subspecies. Kruskal-Wallis test with Dunn's post-hoc correction ( $n$  from left to right (the number of successful copulations in fig. S1B) = 52, 47, 53, and 20).

**(I)** Top row: Competition mating arenas where a male of each *D. mojavensis* subspecies had the choice to court with con-subspecific female or a female of one of the other three subspecies (both are freeze-killed virgin females). Below: Violin plots represent the courtship preference indices of males between females ( $n = 4-5$  replicates), ns  $P > 0.05$ , Wilcoxon signed rank test pairs to zero.

Fig. S2

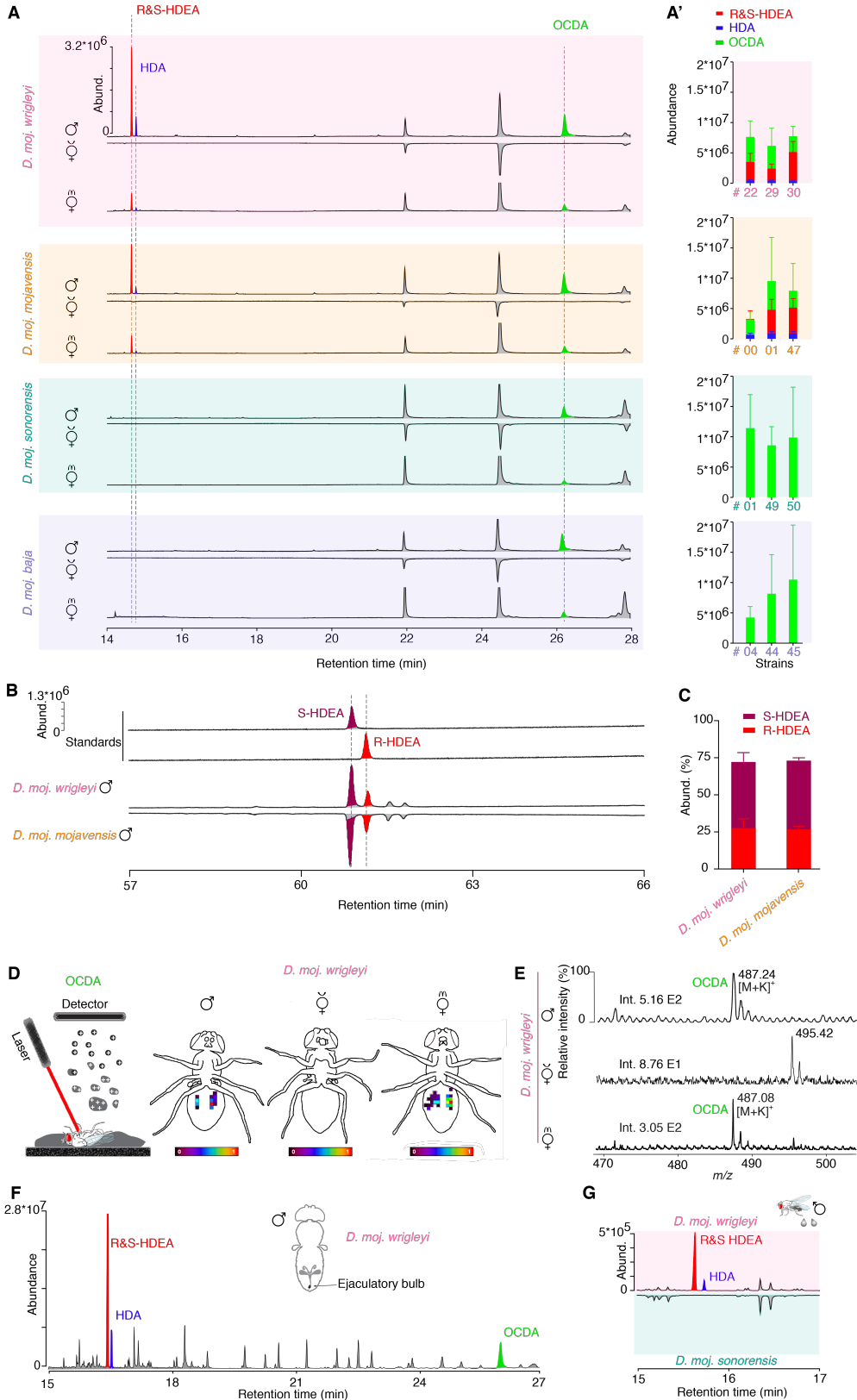


**Fig. S2. Chemical analysis of *D. mojavensis* subspecies.**

**(A)** Representative gas chromatograms of hexane-body wash of 10-day-old male (virgin) and female flies (virgin and mated) ( $n = 5$ ). Colored peaks are the male-transferred compounds during mating; red, R/S-HDEA; blue, HDA; light green, OCDA.

**(A')** Amount of the male-specific compounds in three different strains per each subspecies (*D. moj. wrigleyi*: 15081-1352.22, 15081-1352.29, and 15081-1352.30; *D. moj. mojavensis*: 15081-1352.47, 15081-1352.00, and 15081-1352.01; *D. moj. sonorensis*: 15081-1351.01, 15081-1352.49, and 15081-1352.50; *D. moj. baja*: 15081-1351.04, 15081-1352.44, and 15081-1352.45). Colored bars and error bars indicate mean abundances and SEM of the three male-specific acetates ( $n = 3-4$  males per subspecies).

**(B)** Extracted ion chromatogram of hexane body wash of 10-day-old virgin male at the qualifier ion  $m/z$  236 processed by chiral column ( $n = 3$ ). Colored peaks are S (brown) and R (red) enantiomers of 10Z-heptadecen-2yl acetate.

**(C)** Amount percentage of R and S-HDEA enantiomers in *D. moj. wrigleyi* and *D. moj. mojavensis*. Ns  $P > 0.01$ , Mann Whitney U test ( $n = 3$ ).

**(D)** Representative imaging mass spectrometry for OCDA (see Materials and Methods for details) by MALDI-TOF technique (Left: schematic drawing) of the abdominal surfaces of a 10-day-old male (virgin) and female fly (virgin and mated) ( $n = 3$ ).

**(E)** Representative MALDI-TOF mass spectra of male (virgin) and female flies (virgin and mated) at the qualifier ion  $m/z$  487  $[M+K]^+$  of OCDA.

**(F)** Representative gas chromatogram of ejaculatory bulbs of *D. moj. wrigleyi* obtained by solvent-free TD-GC-MS (Top: schematic drawing) of 10-day-old males (virgin) ( $n = 3$  replicates, each contains 5 ejaculatory bulbs). TD-GC-MS analyses reveal that all three acetates are present in high amounts in the ejaculatory bulb. Colored peaks indicate the male-specific compounds.

**(G)** Gas chromatograms of male-released droplets during courtship in *D. moj. wrigleyi* and *D. moj. sonorensis* ( $n = 3$ ). Chemical analysis revealed the presence of R/S-HDEA and HDA in *D. moj. wrigleyi* droplets but not in droplets of *D. moj. sonorensis*, while OCDA was absent in the droplets of both subspecies. Due to the absence of OCDA signal, the x-axis was shortened. Colored peaks indicate the male-specific acetates (R/S-HDEA and HDA).

Fig. S3

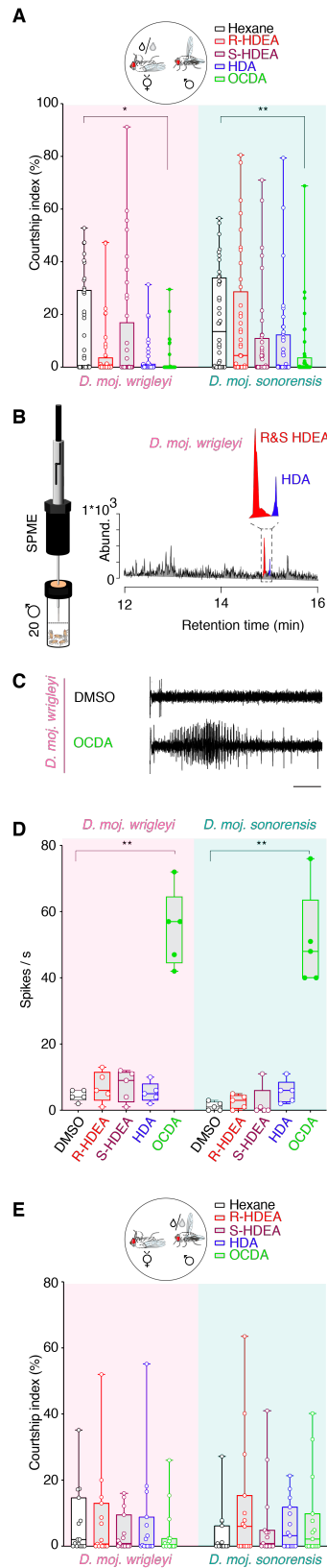


**Fig. S3. OCDA-induce courtship suppression.**

**(A)** Courtship index [%] of males towards dead con-subspecific females perfumed with hexane as a control (black) or one of the male-specific acetates diluted in hexane (colored). Kruskal-Wallis test with Dunn's post-hoc correction. Ns  $P > 0.05$ ; \*  $P < 0.05$ ; \*\*  $P < 0.01$  ( $n = 40$  assays).

**(B)** Headspace collection by SPME (see schematic drawing) and corresponding representative gas chromatogram from 10-day-old males of *D. moj. wrigleyi* trapped inside a mesh (dashed line) in a vial. Enlarged window represents R&S-HDEA (red) and HDA (blue) ( $n = 3$  replicates, each contains 20 males). Due to the absence of OCDA signal, the x-axis was shortened.

**(C)** Representative tip recording traces from foreleg-tarsi using DMSO or OCDA (1  $\mu\text{g}$  diluted in DMSO). Scale bar represents 150 milliseconds (ms).

**(D)** Tip recording measurements from foreleg-tarsi of *D. moj. wrigleyi* and *D. moj. sonorensis* using R or S-HDEA, HDA, OCDA. Ns  $P > 0.05$ ; \*\*  $P < 0.01$ , Kruskal-Wallis test followed by Dunn's multiple comparisons test ( $n = 5$ ).

**(E)** Top: Schematic of courtship arena where a dead virgin female (left, *D. moj. wrigleyi*; right, *D. moj. sonorensis*) is courted by a con-specific male perfumed with hexane or one of the other acetates. Below, y-axis represents courtship index [%] (equal the time a male exhibits courtship behaviors (fig. S1B) / total amount of recording time (10 min)). Ns  $P > 0.05$ , Kruskal-Wallis test followed by Dunn's multiple comparisons test ( $n = 15$ ). Males and females used in this and other panels are 10-day-old.

**Fig. S4**

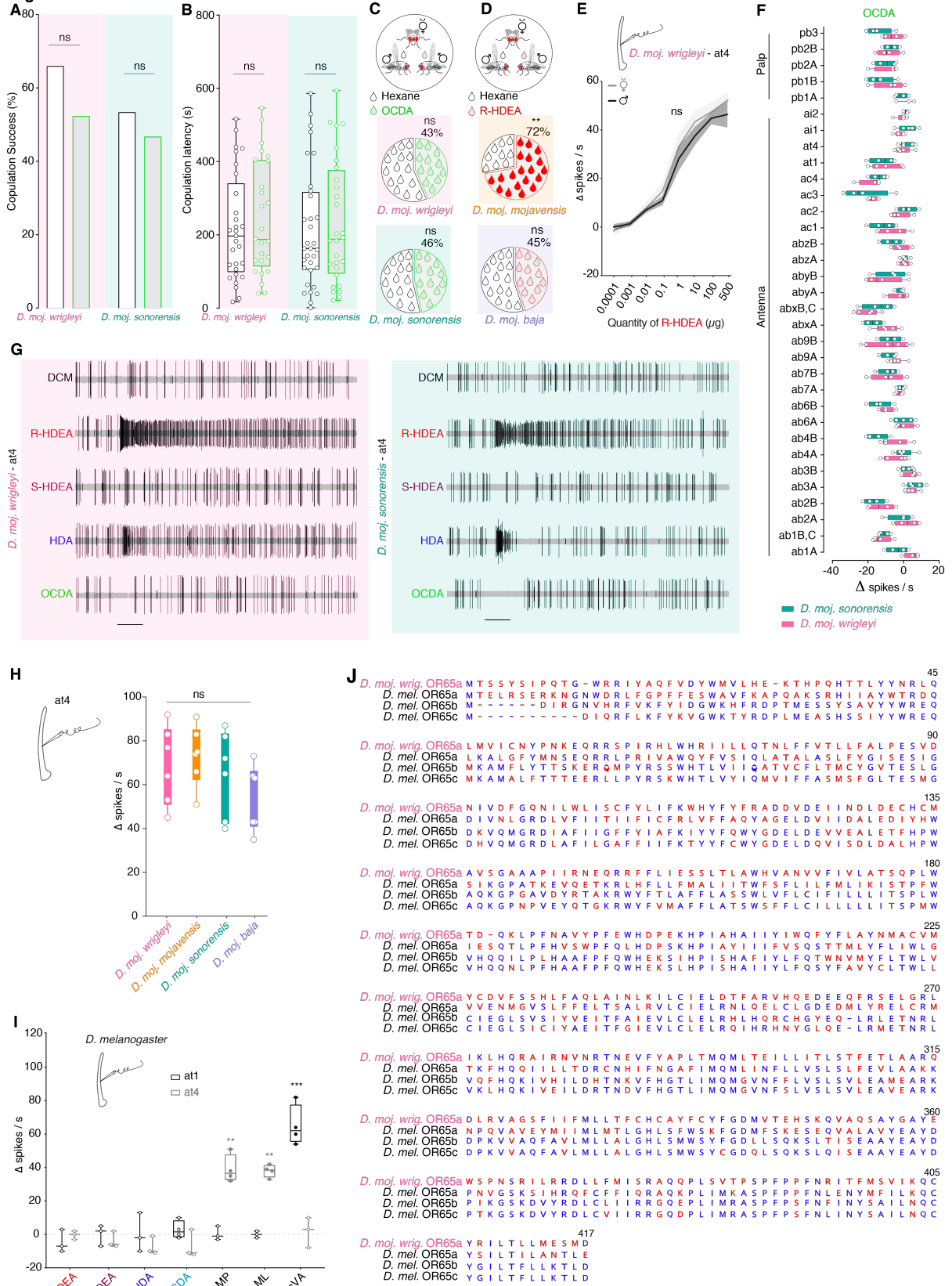


**Fig. S4. Conserved detection mechanism of R-HDEA**

**(A)** Copulation success [%] of *D. moj. wrigleyi* and *D. moj. sonorensis* males performed with hexane or OCDA diluted in hexane ( $n = 40$ ).

- (B)** Copulation latency of the same males perfumed with hexane or OCDA diluted in hexane ( $n$  from left to right = 29, 25, 32, and 28).
- (C)** Competition between two con-subspecific males, perfumed with OCDA or with hexane. See Fig. 4C for details. Ns  $P > 0.05$ , chi-square test ( $n$  from top to bottom = 120 and 112).
- (D)** Top: competition between two males of *D. moj. mojavenensis*, to mate with a virgin female. Bottom: competition between two males of *D. moj. baja*, perfumed with R-HDEA or hexane, to copulate with a virgin con-subspecific female. Ns  $P > 0.05$ ; \*\*  $P < 0.01$ , chi-square test ( $n$  from top to bottom = 100 and 116).
- (E)** Dose-response relationships for at4 neurons of *D. moj. wrigleyi* females (light grey) and males (dark grey) toward R-HDEA (Mean  $\pm$  SEM). Two-way ANOVA followed by Sidak's multiple comparison test between the two sexes responses to the same stimulus, ns  $P > 0.05$  ( $n = 5$  per single dose).
- (F)** Single-sensillum recording (SSR) measurements from all types of olfactory sensilla on antenna and maxillary palp, with OCDA (10  $\mu$ g) as a stimulus. ab, antennal basiconic sensilla; ac, antennal coeloconic; at, antennal trichoid; ai, antennal intermediate; pb, palp basiconic ( $n = 3-6$ ).
- (G)** Representative SSR traces from at4 sensillum of *D. moj. wrigleyi* (red background) and *D. moj. sonorensis* (turquoise background) to DCM (as solvent), R-HDEA, S-HDEA, HDA, and OCDA (100  $\mu$ g). Scale bar represents stimulus duration (0.5 second).
- (H)** Responses of at4 sensilla in *D. mojavenensis* subspecies to R-HDEA (1000  $\mu$ g). Ns  $P > 0.01$ , Kruskal-Wallis test between different treatments with Dunn's post-hoc correction ( $n = 6$ ).
- (I)** Responses of *D. melanogaster* at1 (black) and at4 (grey) to R, HDEA, S-HDEA, HDA, OCDA, methyl palmitate (MP; diagnostic odor for Or88a), methyl laurate (ML; diagnostic odor for Or47b and Or88a) and cVA (diagnostic odor for Or67d neurons) (10  $\mu$ g diluted in DCM). SSR analyses reveal that none of the *D. moj. wrigleyi* male-specific acetates elicited any response in the at1 nor at4 sensillum of *D. melanogaster*. Filled circles in this panel indicate significant difference from solvent responses. Ns  $P > 0.05$ ; \*\*  $P < 0.01$ ; \*\*\*  $P < 0.001$ , Mann Whitney U test ( $n = 3-4$ ).
- (J)** Alignments of *D. moj. wrigleyi*-OR65a and *D. melanogaster*-OR65a/b/c protein sequences. Blue letters represent the similarities while red letters represent the polymorphic sites.

Fig. S5

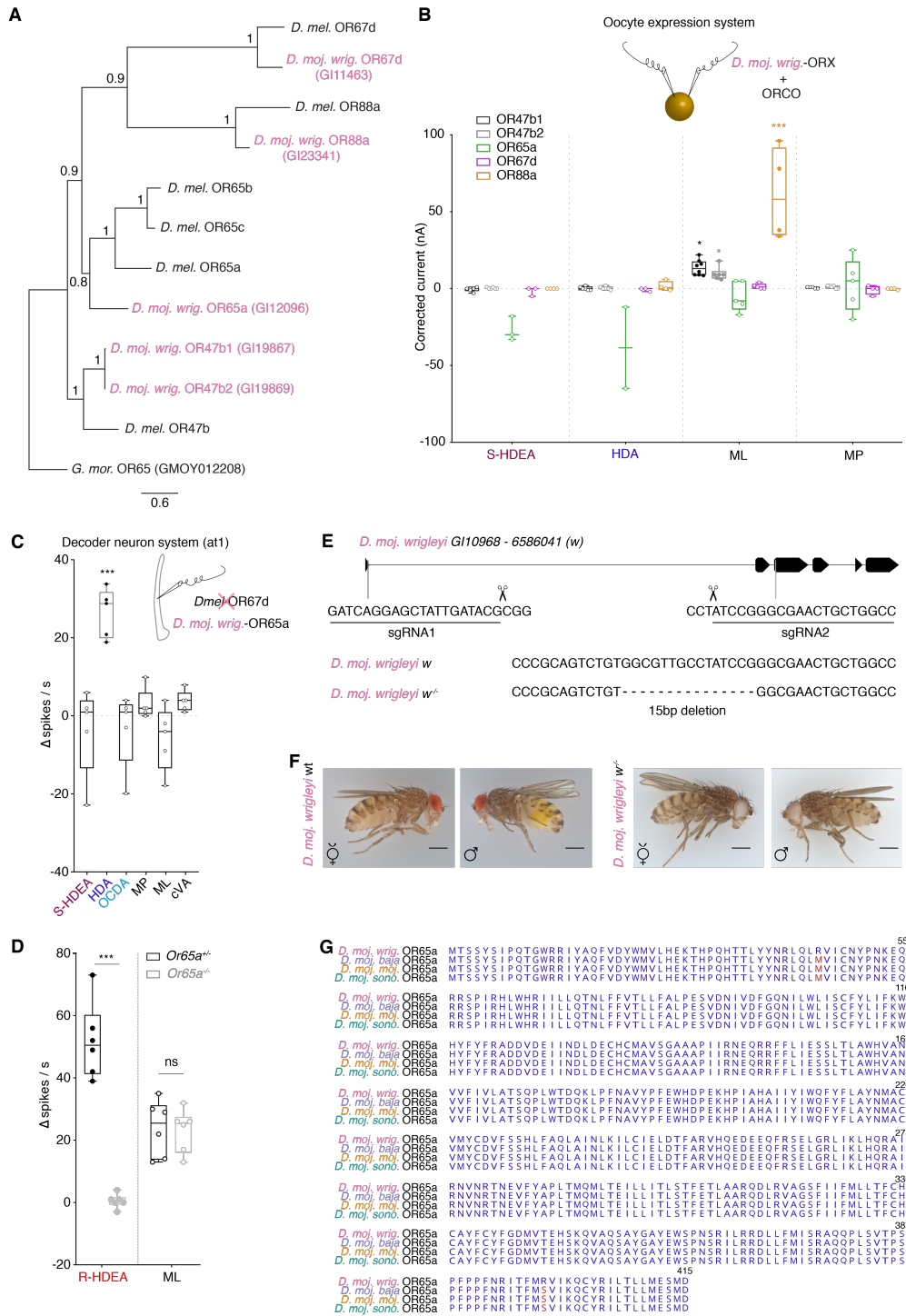


**Fig. S5. Functional characterization of sex pheromone receptors and generation of white mutant flies.**

**(A)** Phylogenetic analysis of pheromone receptors (OR67d, OR88a, OR65 and OR47b) in *D. melanogaster* and *D. moji. wrightleyi* using OR65a ortholog in *Glossina morsitans* as an outgroup. Of the

six pheromone sensing receptors in *D. melanogaster*, five are present in the *D. moj. wrigleyi* genome (11): GI19867 and GI19869 (OR47b1 and OR47b2, respectively), GI12096 (OR65a/b/c), GI11463 (OR67d), and GI23341 (OR88a). GI12096 has three paralogs in *D. melanogaster* (OR65a/b/c) and shares the highest degree of protein alignment with *D. melanogaster*-OR65a (11) compared to others (fig. S4J). The scale bar for branch length represents the number of substitutions per site. Bootstrap values are indicated by the numbers at the nodes.

**(B)** Responses of the five odorant receptors (indicated in different colors), heterologously expressed in *X. laevis* oocytes to S-HDEA, HDA, methyl laurate (diagnostic odor for OR47b), and methyl palmitate (diagnostic odor for OR88a) (1mM diluted in DMSO). Filled circles in this and fig. S5C indicate significant difference from solvent responses, ns  $P > 0.05$ ; \*  $P < 0.05$ ; \*\*\*  $P < 0.001$ , Mann Whitney U test ( $n = 2-8$ ).

**(C)** Responses of the *D. moj. wrigleyi*-Or65a gene heterologously expressed in *D. melanogaster* at1 to previous-mentioned compounds and cis-vaccenyl acetate (diagnostic odor for Or67d) (10  $\mu$ g diluted in DCM). Ns  $P > 0.05$ ; \*\*\*  $P < 0.001$ , Mann Whitney U test ( $n = 3-4$ ).

**(D)** Responses of Or65a heterozygous (black) and homozygous (grey) animals to R-HDEA and methyl laurate (ML) (100  $\mu$ g diluted in DCM). Filled-circles indicate significant difference between both groups. Ns  $P > 0.05$ ; \*\*\*  $P < 0.001$ , Mann Whitney U test ( $n = 6$ ).

**(E)** Schematic drawing of the structure of the *white* gene (GI 10968-6586041) illustrating the strategy for generating knockouts using CRISPR/Cas9. The two guide RNA sequences are shown below; scissors denote the cutting sites. All knock-outs were validated by sequencing the targeted locus in homozygous mutants prior to establishing lines. The *white* gene knockout animals carry a 15 bp deletion.

**(F)** A macrograph of a lateral view of wildtype and *white* mutant female (right) or wildtype and *white* mutant male (left) of *D. moj. wrigleyi*. In addition to the eye color change, the yellowish color of the male's accessory glands disappeared. Scale bar represents 500  $\mu$ m (Photo Credit: V. Grabe, Max Planck Institute for Chemical Ecology).

**(G)** Protein alignment of OR65a in the four *D. moj.* subspecies in an open reading frame. Blue letters represent the similarities while red letters represent the polymorphic sites.

Fig. S6

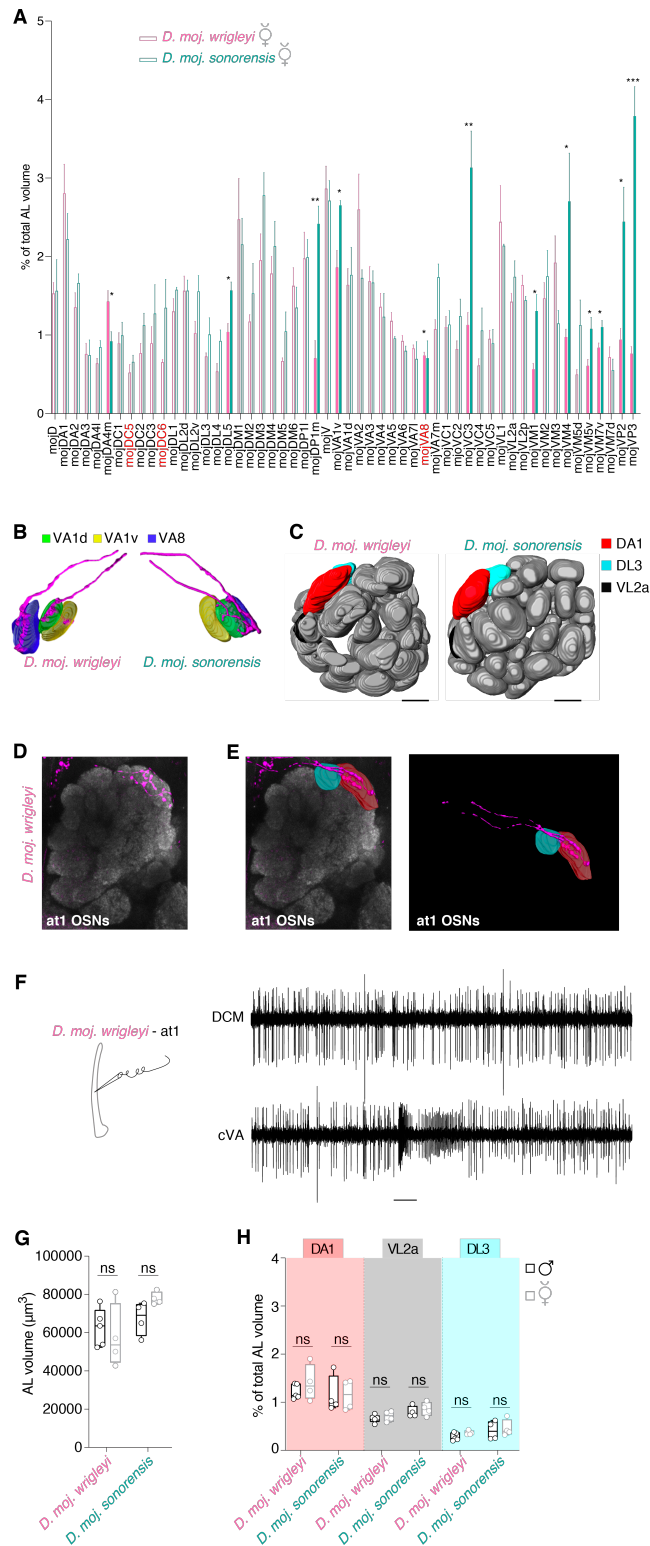


**Fig. S6. Characterization of antennal lobe glomeruli in *D. mojavensis* subspecies.**

(A) Normalized volumes of 54 glomeruli (out of 57, other three glomeruli could be identified but not accessed for volumetric analysis) for *D. moj. wrigleyi* and *D. moj. sonorensis* females. Glomeruli in red

are *D. mojavensis*-specific novel glomeruli, which named according to their relative position to the adjacent glomeruli. Landmark glomeruli (See Materials and Methods) were used as to compare antennal lobes of *D. mojavensis* and *D. melanogaster* as previously used in (54). However, future molecular markers will be necessary to verify this identification. Filled bars indicate significant differences between both subspecies. All data passed Shapiro–Wilk normality test, except the data of DM2, V, and VA2. Normally-distributed data are analyzed by Unpaired t test, otherwise Mann Whitney U test is used. Ns  $P > 0.05$ ; \*  $P < 0.05$ ; \*\*  $P < 0.01$ ; \*\*\*  $P < 0.001$  ( $n = 3-4$  animals per subspecies).

**(B)** A pattern of neurobiotin backfilled neurons (magenta) from at4 sensillum that reveals similar innervation in *D. moj. wrigleyi* (right) and *D. moj. sonorensis* (left) to VA8, VA1v and VA1d glomeruli.

**(C)** Three-dimensional reconstruction of antennal lobes from representative female brains of *D. moj. wrigleyi*, *D. moj. sonorensis* and *D. melanogaster*. DA1, red; DL3, cyan; VL2a, black. Scale bar represents 12  $\mu\text{m}$ .

**(D)** Fluorescent staining for neurobiotin (green) and nc82 (magenta) in *D. moj. wrigleyi* antennal lobe backfilled from at1 sensillum (identified by electrophysiological recordings; Fig. 4E). Backfilling of the at1 sensillum of *D. moj. wrigleyi* revealed a similar innervation target as in *D. melanogaster* (17) to the DA1 glomerulus but with two neuronal tracts innervating separately the anterior and posterior regions of this glomerulus. The backfill image corresponds to a projection of 28 Z-stacks (Watch movie S9).

**(E)** Reconstructions for the backfill signal that innervate the DA1 (red) but not DL3 (cyan) glomerulus.

**(F)** Representative SSR traces from at1 sensillum of *D. moj. wrigleyi* DCM, *cis*-vaccenyl acetate (cVA, 100  $\mu\text{g}$ ). Consistent with the innervation pattern of *D. mojavensis* at1 neurons, SSR analysis of the at1 sensillum revealed the presence of at least two OSNs in this sensillum type similar to (60). Scale bar represents the stimulus duration (0.5 s).

**(G)** Antennal lobe volumes ( $\mu\text{m}^3$ ) for males (black) and females (grey) of *D. moj. wrigleyi* and *D. moj. sonorensis*. Filled circles in this and below panels indicate significant difference from the other sex within the same species, ns  $P > 0.05$ ; \*  $P < 0.05$ ; \*\*  $P < 0.01$ , Mann Whitney U test ( $n = 4-6$ ).

**(H)** Normalized volumes of DA1, VL2a and DL3 for *D. moj. wrigleyi* and *D. moj. sonorensis* females and males.

Fig. S7

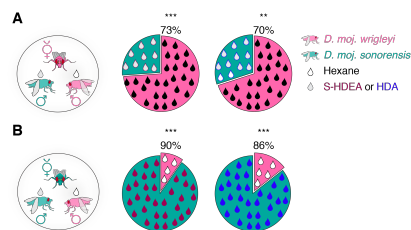


**Fig. S7. S-HDEA and HDA are not involved in sexual isolation among *D. mojavensis* subspecies.**

**(A)** Competition between two males of different subspecies, *D. moj. sonorensis* male perfumed with S-HDEA (brown droplet, left panel) or HDA (blue droplet, right panel) and *D. moj. wrigleyi* male perfumed with hexane (black droplets), to copulate with *D. moj. wrigleyi* virgin female. Pie-charts in A-B represent copulation success [%] of the rival males, \*\*  $P < 0.01$ ; \*\*\*  $P < 0.001$ , chi-square test ( $n$  from left to right = 92 and 80, respectively). All males and females used in this and other panels were 10-day-old virgin flies.

**(B)** Competition between two males of different subspecies, *D. moj. sonorensis* male perfumed with S-HDEA (brown droplet, left panel) or HDA (blue droplet, right panel) and *D. moj. wrigleyi* male perfumed with hexane (black droplets), to copulate with *D. moj. sonorensis* virgin female. ( $n$  from left to right = 84 for both panels).

Table S1

REAGENT or RESOURCE	SOURCE	IDENTIFIER
<b>Experimental Models: Species or strains (<i>Drosophila</i>) and Breeding medium</b>		
<i>D. melanogaster</i> , Canton-S strain (Cornmeal food)	NA	NA
<i>D. melanogaster</i> ; <i>y w M(eGFP.vas-int.Dm)ZH-2A; M(RFP.attP)ZH-51D</i> ; +; + (Cornmeal food)	FlyC31	ΦX-51D
<i>D. melanogaster</i> , <i>y w; Bl/CyO; TM2/TM6B</i> (Cornmeal food)	Lindsely and Zimm, 1992	NA
<i>D. melanogaster</i> , <i>w-; Bl/CyO; D.mel-Or67d<sup>Gal4</sup>/TM6B</i> (Cornmeal food)	Kurtovic, 2007	NA
<i>D. melanogaster</i> , <i>w-; UAS-D.moj.wirg.-Or47b1; D.mel-Or67d<sup>Gal4</sup></i> (Cornmeal food)	This paper	NA
<i>D. melanogaster</i> , <i>w-; UAS-D.moj.wirg.-Or47b2; D.mel-Or67d<sup>Gal4</sup></i> (Cornmeal food)	This paper	NA
<i>D. melanogaster</i> , <i>w-; UAS-D.moj.wirg.-Or65a; D.mel-Or67d<sup>Gal4</sup></i> (Cornmeal food)	This paper	NA
<i>D. melanogaster</i> , <i>w-; UAS-D.moj.wirg.-Or67d; D.mel-Or67d<sup>Gal4</sup></i> (Cornmeal food)	This paper	NA
<i>D. melanogaster</i> , <i>w-; UAS-D.moj.wirg.-Or88a; D.mel-Or67d<sup>Gal4</sup></i> (Cornmeal food)	This paper	NA
<i>D. melanogaster</i> , <i>w-; UAS-D.moj.sono.-Or65a; D.mel-Or67d<sup>Gal4</sup></i> (Cornmeal food)	This paper	NA
<i>D. mojavensis wrightleyi</i> (Banana food)	NDSSC	15081-1352.22
<i>D. mojavensis wrightleyi</i> (Banana food)	NDSSC	15081-1352.29
<i>D. mojavensis wrightleyi</i> (Banana food)	NDSSC	15081-1352.30
<i>D. mojavensis baja</i> (Banana food)	NDSSC	15081-1351.04
<i>D. mojavensis baja</i> (Banana food)	NDSSC	15081-1352.44
<i>D. mojavensis baja</i> (Banana food)	NDSSC	15081-1352.45
<i>D. mojavensis mojavensis</i> (Banana food)	NDSSC	15081-1352.47
<i>D. mojavensis mojavensis</i> (Banana food)	NDSSC	15081-1352.00
<i>D. mojavensis mojavensis</i> (Banana food)	NDSSC	15081-1352.01
<i>D. mojavensis sonorensis</i> (Banana food)	NDSSC	15081-1351.01
<i>D. mojavensis sonorensis</i> (Banana food)	NDSSC	15081-1352.49
<i>D. mojavensis sonorensis</i> (Banana food)	NDSSC	15081-1352.50
<i>D. moj. wrightleyi Or65a<sup>-/-</sup></i> (Banana food)	This paper	NA
<i>D. moj. wrightleyi w<sup>-/-</sup></i> (Banana food)	This paper	NA
<b>Chemicals and their Diagnostic Uses</b>		
Isopropyl benzoate (ab1A, ab2B)	Sigma-Aldrich	94-46-2

Dimethyl disulfide (ab1B)	Sigma-Aldrich	624-92-0
Hexyl acetate (ab3A, ab7A)	Sigma-Aldrich	142-92-7
Isopentyl acetate (ab4A)	Sigma-Aldrich	123-92-2
Geosmin (ab4B)	Sigma-Aldrich	16423-19-1
Guaiacol (ab6B)	Sigma-Aldrich	90-05-1
Ethyl lactate (ab7B)	Sigma-Aldrich	97-64-3
Acetophenone (ab9B)	Sigma-Aldrich	98-86-2
1-hexanol (abzB)	Merck	111-27-3
Ethyl 3-hydroxybutyrate (abxB)	Fluka	5405-41-4
4-ethylguaiacol (pb1B)	Sigma-Aldrich	2785-89-9
(-)-fenchone (pb2A)	Sigma-Aldrich	7787-20-4
2-heptanone (pb3B)	Sigma-Aldrich	110-43-0
Ammonia (ac1)	Sigma-Aldrich	7664-41-7
1,4-Diaminobutane (ac2)	Sigma-Aldrich	110-60-1
1-octanol (ac3)	Sigma-Aldrich	111-87-5
Phenylacetaldehyde (ac4)	Sigma-Aldrich	122-78-1
Farnesol (ai1)	Sigma-Aldrich	4602-84-0
Valencene (ai2)	Sigma-Aldrich	4630-07-3
<i>cis</i> -vaccenyl acetate (at1 and Oocyte experiments)	Biomol	6186-98-7
Methyl laurate (at4 and Oocyte experiments)	Fluka	111-82-0
Methyl palmitate (at4 and Oocyte experiments)	Sigma-Aldrich	112-39-0
Dichloromethane (DCM, Solvent for SSR experiments)	Sigma-Aldrich	75-09-2
Hexane (Hex, Solvent for Behavioral experiments)	Sigma-Aldrich	110-54-3
Dimethyl sulfoxide (DMSO, Solvent for Oocyte experiments)	Sigma-Aldrich	200-664-3
( <i>R,Z</i> )-10-Heptadecen-2-ylacetate (R-HDEA)	This paper	NA
( <i>S,Z</i> )-10-Heptadecen-2-ylacetate (S-HDEA)	This paper	NA
Heptadec-2-yl acetate (HDA)	This paper	NA
(19 <i>Z</i> ,22 <i>Z</i> )- Octacosadienyl acetate (OCDA)	This paper	NA
<b>Oligonucleotides and their targets (BamHI site, Kozaq sequence, and XbaI site)</b>		
<i>Orco</i> Fwd, (to amplify from cDNA) ATGGCTACATCAATGCAGCCCGGCAAG	This paper	NA
<i>Orco</i> Rev, (to amplify from cDNA) TCACTTGAGTTGCACCAGCAC	This paper	NA
<i>Orco</i> Fwd, (to clone in pCS2+ vector) CGCGGATCCGCCACCATGGCTACATCAATGCAGCCCGGC AAG	This paper	NA
<i>Orco</i> Rev, (to clone in pCS2+ vector) GCTCTAGATCACTTGAGTTGCACCAGCAC	This paper	NA
<i>Or47b</i> Fwd, (to amplify from cDNA) ATGGCCAATGGGGATTTCAAG	This paper	NA
<i>Or47b</i> Rev, (to amplify from cDNA) TTACATGGCCTCACGCAGCA	This paper	NA

Or47b Fwd, (to clone in pCS2+ vector) CGCGGATCCGCCACCATGGCCAATGGGGATTTC AAG	This paper	NA
Or47b Rev, (to clone in pCS2+ vector) GCTCTAGATTACATGGCCTCACGCAGCA	This paper	NA
Or65a Fwd, (to amplify from cDNA) ATGACGAGCAGCTATAGTATAC	This paper	NA
Or65a Rev, (to amplify from cDNA) TTAATCCATGCTCTCCATCAAG	This paper	NA
Or65a Fwd, (to clone in pCS2+ vector) CGCGGATCCGCCACCATGACGAGCAGCTATAGTATAC	This paper	NA
Or65a Rev, (to clone in pCS2+ vector) GCTCTAGATTAATCCATGCTCTCCATCAAG	This paper	NA
Or67d Fwd, (to amplify from cDNA) ATGGCGAAGACGGCTGTG	This paper	NA
Or67d Rev, (to amplify from cDNA) TTATATCTCGTAGTCCAAGTACGTAATCATC	This paper	NA
Or67d Fwd, (to clone in pCS2+ vector) CGCGGATCCGCCACCATGGCGAAGACGGCTGTG	This paper	NA
Or67d Rev, (to clone in pCS2+ vector) GCTCTAGATTATATCTCGTAGTCCAAGTACGTAATCATC	This paper	NA
Or88a Fwd, (to amplify from cDNA) ATGGATAACATAAATCAACCCA	This paper	NA
Or88a Rev, (to amplify from cDNA) CTATTGTCGTGACTTGAGAAATGTG	This paper	NA
Or88a Fwd, (to clone in pCS2+ vector) CGCGGATCCGCCACCATGGATAACATAAATCAACCCA	This paper	NA
Or88a Rev, (to clone in pCS2+ vector) GCTCTAGACTATTGTCGTGACTTGAGAAATGTG	This paper	NA
Guide sequence 1 for <i>D. moj. white</i> (w sgRNA1), GGCCAGCAGTTCGCCCGGAT	This paper	NA
Or47b Fwd (to amplify RNA <i>in situ</i> probe), ATCGCGATTTGCCCTACCAT	This paper	NA
Or47b Rev (to amplify RNA <i>in situ</i> probe), AGCTCTTACATGGCCTCACG	This paper	NA
Or65a Fwd (to amplify RNA <i>in situ</i> probe), TGGACTACTGGATGGTGCTG	This paper	NA
Or65a Rev (to amplify RNA <i>in situ</i> probe), TTAATCCATGCTCTCCATCAAG	This paper	NA
Or67d Fwd (to amplify RNA <i>in situ</i> probe), ATGGCGAAGACGGCTGTG	This paper	NA
Or67d Rev (to amplify RNA <i>in situ</i> probe), TTATATCTCGTAGTCCAAGTACGTAATCATC	This paper	NA
Or88a Fwd (to amplify RNA <i>in situ</i> probe), GTATTGTCAACAGATCGG	This paper	NA
Or88a Rev (to amplify RNA <i>in situ</i> probe), TCGCATAGCACATTGATC	This paper	NA
Guide sequence 2 for <i>D. moj. white</i> (w sgRNA2), GATCAGGAGCTATTGATACG	This paper	NA
w sgRNA1 genotyping Fwd, CGAGCCAATGAACAGATCGTCCT	This paper	NA
w sgRNA1 genotyping Rev, GAACTATGGCACGCTGAGTCCT	This paper	NA

w sgRNA2 genotyping Fwd, CGGTTTCTAGGCATGTCAATACAC	This paper	NA
w sgRNA2 genotyping Rev, GCCTTGCTCCATAAGTAAATAGCT	This paper	NA
Guide sequence 1 for <i>D. moj. Or65a</i> (Or65a sgRNA1), CAGCACACCACGCTCTATTA	This paper	NA
Guide sequence 2 for <i>D. moj. Or65a</i> (Or65a sgRNA2), CGCTCTATTATAATCGGCTG	This paper	NA
Or65a sgRNA1+2 genotyping Fwd, GCGCAATTCGTGGACTACTGGATGG	This paper	NA
Or65a sgRNA1+2 genotyping Rev, GCGCTGCTCCTTGTCGGATAGTTGC	This paper	NA
<b>Software</b>		
Noldus	Noldus	<a href="https://www.noldus.com">https://www.noldus.com</a>
ChemStation (F.1.3.2357)	Agilent	<a href="https://www.agilent.com/">https://www.agilent.com/</a>
NIST Mass spectra Search Program (v2.2)	NIST	<a href="https://www.nist.gov">https://www.nist.gov</a>
ChemDraw Professional (v17.1)	Chem Office 2017	<a href="https://www.perkinelmer.com/">https://www.perkinelmer.com/</a>
MassLynx (v4.0)	Waters	<a href="https://www.waters.com">https://www.waters.com</a>
BioMap	MS Imaging	<a href="https://ms-imaging.org">https://ms-imaging.org</a>
Geneious (11.0.5)	Geneious	<a href="https://www.geneious.com">https://www.geneious.com</a>
ImageJ (Fiji)	NIH	<a href="https://imagej.net/Fiji">https://imagej.net/Fiji</a>
Zen (2)	Zeiss	<a href="https://www.zeiss.com">https://www.zeiss.com</a>
NIS Elements Viewer (v4.5)	Nikon	<a href="https://www.nikon.com">https://www.nikon.com</a>
AMIRA (v5.6.0)	Visualization Sciences Group	<a href="http://www.vsg3d.com">http://www.vsg3d.com</a>
AutoSpike (v3.7)	Synteck	<a href="http://www.ockenfels-syntech.com">http://www.ockenfels-syntech.com</a>
Cellworks	npielectronic	<a href="http://www.npielectronic.de/home.html">http://www.npielectronic.de/home.html</a>
Tilde	Bas van Steensel lab	<a href="https://tide.deskgen.com">https://tide.deskgen.com</a>
GraphPad Prism (v8.2)	GraphPad	<a href="https://www.graphpad.com">https://www.graphpad.com</a>
Rstudio (v1.1.447)	R Consortium	<a href="https://www.r-project.org">https://www.r-project.org</a>
Illustrator (v23.1.1)	Adobe	<a href="http://www.adobe-students.com">http://www.adobe-students.com</a>

**Table S1. List of *Drosophila* socks, chemicals, oligonucleotides, and software used in the study.**

**Movie S1. Sexual behaviors of *D. mojavensis wrightleyi*.**

During the first minute, most males of the four subspecies were eager to court by orienting and following the females. Subsequently, males tapped the females' bodies with their forelegs, followed by wing spreading and fanning for vibrational song production. Females responded to the males' song by vibrating their wings. Males followed the females by extending their proboscis to lick the females' genitalia and then attempted copulation. Males while courting the female in addition released a fluidic droplet from their anus. We called this novel trait "dropping behavior". In response to the rapid male courtship elements, females slow down their movement, quiver their abdomen, vibrate their wings and scissor them as signs for acceptance, while kicking with legs or accelerating the movement speed to signal rejection.

**Movie S2. Sexual behaviors of *D. moj. mojavensis*.**

**Movie S3. Sexual behaviors of *D. moj. sonorensis*.**

**Movie S4. Sexual behaviors of *D. moj. baja*.**

**Movie S5. 3-D reconstruction of *D. moj. wrightleyi* antennal lobe (female).**

**Movie S6. 3-D reconstruction of *D. moj. sonorensis* antennal lobe (female).**

**Movie S7. Neurobiotin backfilled neurons from at4 sensillum in *D. moj. wrightleyi*.**

Fluorescent staining for neurobiotin (green) and nc82 (magenta) of *D. moj. wrightleyi* antennal lobe, backfilled from at4 sensillum.

**Movie S8. Neurobiotin backfilled neurons from at4 sensillum in *D. moj. sonorensis*.**

Fluorescent staining for neurobiotin (green) and nc82 (magenta) of *D. moj. sonorensis* antennal lobe, backfilled from at4 sensillum.

**Movie S9. Neurobiotin backfilled neurons from at1 sensillum in *D. moj. wrightleyi*.**

Fluorescent staining for neurobiotin (green) and nc82 (magenta) of *D. moj. wrightleyi* antennal lobe, backfilled from at1 sensillum.

**Data file S1.** Sequence alignments of *Or47b1* and *Or47b2* loci in *D. moj. wrightleyi* (provided as Fasta file).

## Text S1

### Chemical identification and synthesis

#### Chemical identification

TDU-GC/EIMS data obtained from virgin males and females show three chromatographic peaks abundant in males. The first one (KI 1998) was the most abundant. Molecular ion peak is not visible, but rather  $m/z$  236 is abundant. Accurate mass provided molecular composition  $C_{17}H_{32}$ . A large EE ion series of 194 (236- $C_3H_6$ ), 180, 166 up to 82 (consecutive losses of  $CH_2$ ) indicate unsaturation in alicyclic chain. Diagnostic peaks at  $m/z$  87 ( $\alpha$ -cleavage,  $C_4H_7O_2$ ), 61 ( $C_2H_3O_2$ ) 43 indicate acetyl group on position 2. Then  $m/z$  236 peak represents  $[M-CH_3COOH]^+$ . The double bond position was determined by converting the compound to dimethyldisulfite (DMDS) adduct. The EIMS spectrum show  $m/z$  390  $[M]^+$  and indicative fragments A:  $m/z$  245 and  $m/z$  185  $[A-CH_3COOH]^+$ ; B: 145 plus additional ions at  $m/z$  87 and 61. Data analysis suggests 10-heptadecen-2-yl-acetate. The prepared (*rac*,10*Z*)-heptadecen-2-yl-acetate (HDEA) show undistinguishable EIMS spectra and chromatographic retention as the natural product. Chirality and enantiomeric purity of natural acetate was determined on a chiral GC column using prepared (2*R*,10*Z*)-heptadecen-2-yl-acetate and (2*R*,10*Z*)-heptadecen-2-yl-acetate standards.

The second peak with longer retention (KI 2017) show in EIMS spectrum low-abundant molecular ion  $m/z$  298  $M^+$ ,  $m/z$  256  $[M-C_2H_2O]^+$  and intense  $m/z$  238  $[M-CH_3COOH]^+$ . In addition, OE ion series from  $m/z$  153-55 separated by 14Da and peaks at  $m/z$  87 ( $\alpha$ -cleavage,  $C_4H_7O_2$ ), 61 ( $C_2H_3O_2$ ) 43 indicating saturated aliphatic chain and acetyl group on position 2. The second peak is heptadec-2-yl-acetate (HDA). HDA have also chiral center at position 2, however 2*R*- and 2*S*-enantiomers were present in 50/50 ratio and only and *rac*-heptadec-2-yl-acetate was prepared and further used in this study.

Third peak with much longer retention (KI 3058) shows in abundant molecular ion  $m/z$  448 ( $M^+$ , accurate mass  $m/z$  448.42951 for  $C_{30}H_{56}O_2$  calculated 448.428032) and fragment ions at  $m/z$  405  $[M-C_2H_2O]^+$  and  $m/z$  388  $[M-CH_3COOH]^+$  accompanied with EE ion series from  $m/z$  264-166 OE series  $m/z$  149-67 both spaced by 14Da. Acetate function was deduced from  $m/z$  61 ( $C_2H_3O_2$ ) most probably in position 1. Intense ions  $m/z$  149, 135, 121 and 109 indicate omega-6 and omega-9 skipped diene structure. Data suggest (*Z,Z*)-19,22-octacosadien-1-yl acetate (OCDA) as the third peak and the proposed structure was confirmed by chemical synthesis.

#### Chemical synthesis

Commercially available chemicals were used without further purification. Tetrahydrofuran (anhydrous, Sigma-Aldrich) and dichloromethane (Roth) were used as received. All reactions except the enzymatic hydrolysis were carried out under an atmosphere of argon. Preparative column chromatography was performed on Silica gel 60 (230-400 mesh, Carl Roth GmbH) and TLC analysis on commercial Merck silica gel 60 F<sub>254</sub> plates. NMR spectra were measured on a Bruker Avance 400 NMR spectrometer. Chemical shifts are reported in ppm downfield from TMS.

#### Synthesis of (*R*) and (*S,Z*)-10-Heptadecen-2-ylacetate (*R&S*-HDEA).

##### *Synthesis of (Z)-10-Heptadecen-2-one.*

Palmitoleic acid (250 mg, 0.98 mmol) was dissolved in 10 mL of THF and cooled to  $-78^\circ\text{C}$ . A 1.6 M solution of MeLi in diethylether (1.53 ml, 2.45 mmol) was added dropwise and the mixture was allowed to warm to room temperature by removing the cooling bath. The reaction was monitored via TLC. Upon completion (after ca. 2.5h) the mixture was poured into 20 mL of 1N HCl at  $0^\circ\text{C}$  and extracted with diethylether (3x15 ml). The combined organic layers were washed with saturated  $\text{NaHCO}_3$  (20 ml) and brine (20 ml), dried with anhydrous  $\text{NaSO}_4$ , filtered and concentrated in vacuo. After purification via silica gel column chromatography (12:1 hexane/EtOAc) (*Z*)-10-Heptadecen-2-one was obtained as colourless oil (225 mg, 91%).  $^1\text{H-NMR}$ : (400 MHz,  $\text{CDCl}_3$ )  $\delta$  = 5.35 (m, 2H), 2.41 (t,  $J$  = 7.3 Hz, 2H), 2.13 (s, 3H), 2.01 (q,  $J$  = 5.7 Hz, 4H), 1.57 (m, 2H), 1.29 (m, 16H), 0.89 (t,  $J$  = 6.0 Hz, 3H)ppm;  $^{13}\text{C-NMR}$ : (100 MHz,  $\text{CDCl}_3$ )  $\delta$  = 209.2, 130.0, 129.7, 43.8, 31.8, 29.8, 29.72, 29.68, 29.28, 29.15, 29.09, 28.97, 27.22, 27.15, 23.9, 22.6, 14.1 ppm.

##### *Synthesis of ( $\pm$ )-10-Heptadecen-2-yl acetate.*

(*Z*)-10-Hexadecen-2-one (100 mg, 0.4 mmol) was dissolved in 20 mL of Ethanol and 15 mg NaBH<sub>4</sub> (0.4 mmol) were added. The mixture was stirred at room temperature and after 45 min 5 mL sat. NH<sub>4</sub>Cl solution was added. The mixture was extracted with diethylether (3x15 ml). The combined organic layers were washed with water (20 ml) and brine (20 ml), dried with anhydrous NaSO<sub>4</sub>, filtered and concentrated in vacuo to obtain crude (*Z*)-10-Heptadecen-2-ol. The alcohol was dissolved in 10 mL CH<sub>2</sub>Cl<sub>2</sub> and 100  $\mu$ l Ac<sub>2</sub>O, 100  $\mu$ l NEt<sub>3</sub> and 2 crystals of DMAP were added. The mixture was stirred at room temperature overnight, quenched with 10 ml water and extracted with diethylether (3x15 ml). The combined organic layers were washed with brine (20 mL), dried with anhydrous NaSO<sub>4</sub>, filtered and concentrated in vacuo. Purification via silica gel column chromatography (12:1 hexane/EtOAc) yielded racemic (*Z*)-10-Heptadecen-2-yl acetate as colourless oil (115 mg, 97%). <sup>1</sup>H-NMR: (400 MHz, CDCl<sub>3</sub>)  $\delta$  = 5.35 (m, 2H), 4.88 (hex, *J* = 6.3 Hz, 2H), 2.03 (s, 3H), 2.01 (q, *J* = 6.2 Hz, 4H), 1.51 (m, 2H), 1.29 (m, 18H), 1.20 (d, *J* = 6.4 Hz, 3H), 0.89 (t, *J* = 6.8 Hz, 3H) ppm; <sup>13</sup>C-NMR: (100 MHz, CDCl<sub>3</sub>)  $\delta$  = 170.8, 130.0, 129.8, 71.1, 35.9, 31.8, 29.7, 29.4, 29.2, 29.0, 27.22, 27.15, 25.4, 22.6, 21.4, 19.9, 14.1 ppm; EI-MS [m/z (relative intensity)]: 41 (58), 43 (100), 54 (45), 55 (84), 67 (63), 68 (51), 69 (57), 81 (67), 82 (89), 83 (40), 95 (63), 96 (77), 97 (23), 109 (33), 110 (38), 124 (49), 138 (38), 152 (12), 166 (8), 180 (5), 194 (7), 236 (35), 281 (4 [M-CH<sub>3</sub>]<sup>+</sup>).

#### *Separation of (R)- and (S,Z)-10-Heptadecen-2-yl acetate.*

100 mg of ( $\pm$ )-10-Heptadecen-2-yl acetate were dissolved in 1 mL of acetone and 7 mL of phosphatebuffer (0,1M, pH = 7.0) were added to create a fine suspension. Immobilized lipase from *Candida antarctica* was added (40 mg, 2,9 U/mg) and the mixture was stirred at room temperature. The reaction was monitored via GC-MS using a chiral column (Cyclodex B, Agilent). After 20 h the mixture was extracted with diethylether (3x10 ml), washed with brine (10 ml), dried with anhydrous NaSO<sub>4</sub>, filtered and concentrated in vacuo. Purification via silica gel column chromatography (9:1 hexane/EtOAc) yielded pure (*R,Z*)-10-Heptadecen-2-ol (27 mg) and (*Z*)-10-Heptadecen-2-yl acetate (67 mg of a 3:1 mixture of the (*S*)- and (*R*)-enantiomer). (*R,Z*)-10-Heptadecen-2-ol was reacylated using the same protocol as described before to give (*R,Z*)-10-Heptadecen-2-yl acetate (25mg, ee = 99%, optical rotation:  $[\alpha]^{20}_{589} = +1.3$ , 3.01 mg/mL hexane). The remaining mixture of the (*S*) and (*R*)-enantiomer was again subjected to enzymatic hydrolysis until all of the remaining (*R*)-enantiomer was hydrolysed (ca. 48h). The mixture was worked up as described before and purified via silica gel column chromatography (9:1 hexane/EtOAc) to obtain (*S,Z*)-10-Heptadecen-2-yl acetate (31 mg, ee = 97.5%, optical rotation:  $[\alpha]^{20}_{589} = -1.4$ , 3.55 mg/mL hexane ).

### **Synthesis of Heptadec-2-yl acetate (HDA)**

#### *Synthesis of Heptadecan-2-one.*

Palmitic acid (1.6 g, 6.25 mmol) was dissolved in 25 mL of THF and cooled to -78°C. A 1.6 M solution of MeLi in diethylether (8.6 ml, 13.75 mmol) was added dropwise and the mixture was allowed to warm to room temperature by removing the cooling bath. The reaction was monitored via TLC. Upon completion (after ca. 2.5h) the mixture was poured into 40 mL of 1N HCl at 0°C and extracted with diethylether (3x40 ml). The combined organic layers were washed with saturated NaHCO<sub>3</sub> (50 ml) and brine (50 ml), dried with anhydrous NaSO<sub>4</sub>, filtered and concentrated in vacuo. After purification via silica gel column chromatography (12:1 hexane/EtOAc) Heptadecan-2-one was obtained as white wax (1.4 g, 90%). <sup>1</sup>H-NMR: (400 MHz, CDCl<sub>3</sub>)  $\delta$  = 2.41 (t, *J* = 7.5 Hz, 2H), 2.13 (s, 3H), 1.57 (m, 2H), 1.29 (m, 26H), 0.89 (t, *J* = 6.8 Hz, 3H) ppm; <sup>13</sup>C-NMR: (100 MHz, CDCl<sub>3</sub>)  $\delta$  = 209.4, 43.8, 31.9, 29.8, 29.7, 29.7, 29.6, 29.5, 29.4, 29.3, 29.2, 23.9, 22.7, 14.1 ppm.

#### *Synthesis of ( $\pm$ )-Heptadecan-2-ol.*

Heptadecan-2-one (1.35 g, 5.3 mmol) was dissolved in 100 mL of ethanol and NaBH<sub>4</sub> (0.8 g, 21 mmol) was added at 0°C. The mixture was stirred for 2h at room temperature, quenched with 50 mL of sat. NH<sub>4</sub>Cl-solution diluted with 50 mL water and extracted with diethylether (2x100 ml). The combined organic layers were washed with saturated NaHCO<sub>3</sub> (50 ml) and brine (50 ml), dried with anhydrous NaSO<sub>4</sub>, filtered and concentrated in vacuo. The residue was chromatographed on silica gel (9:1 hexane/EtOAc) to yield ( $\pm$ )-Heptadecan-2-ol as a white wax (1.2 g, 88%). <sup>1</sup>H-NMR: (400 MHz, CDCl<sub>3</sub>)  $\delta$  = 3.78 (h, *J* = 5.9 Hz, 1H), 1.20-1.52 (m, 28H), 1.18 (t, *J* = 5.9 Hz, 3H), 0.88 (d, *J* = 6.6 Hz, 3H)ppm; <sup>13</sup>C-

NMR: (100 MHz, CDCl<sub>3</sub>)  $\delta$  = 68.2, 39.4, 31.9, 29.67, 29.64, 29.61, 29.60, 29.3, 25.8, 23.5, 22.7, 14.1 ppm.

#### *Synthesis of ( $\pm$ )-Heptadec-2-yl acetate.*

( $\pm$ )-Heptadecan-2-ol (1.17 g, 4.6 mmol) was dissolved in 20 mL CH<sub>2</sub>Cl<sub>2</sub> and 940  $\mu$ L Ac<sub>2</sub>O, 1.4 mL NEt<sub>3</sub> and 20 mg of DMAP were added. The mixture was stirred at room temperature for 3h, quenched with 20 mL ice-water and extracted with diethylether (3x30 ml). The combined organic layers were washed with water (40 ml) and brine (40 ml), dried with anhydrous NaSO<sub>4</sub>, filtered and concentrated in vacuo. Purification via silica gel column chromatography (12:1 hexane/EtOAc) yielded ( $\pm$ )-Heptadec-2-yl acetate as a white wax (1.36 g, 99%). <sup>1</sup>H-NMR: (400 MHz, CDCl<sub>3</sub>)  $\delta$  = 4.88 (h,  $J$  = 6.3 Hz, 1H), 2.02 (s, 3H), 1.51 (m, 2H), 1.20-1.37 (m, 26H), 1.20 (d,  $J$  = 6.3 Hz, 3H), 0.88 (t,  $J$  = 6.8 Hz, 3H)ppm; <sup>13</sup>C-NMR: (100 MHz, CDCl<sub>3</sub>)  $\delta$  = 170.5, 71.1, 35.9, 31.9, 29.68, 29.65, 29.61, 29.57, 29.53, 29.45, 29.35, 25.4, 22.7, 21.4, 19.9, 14.1 ppm; EI-MS data in agreement with data from Wiley Subscription Services, Inc. (US) via SciFinder.

#### **Synthesis of (19Z,22Z)- Octacosadienyl acetate (OCDA).**

##### *Synthesis of 3-Eicosyn-1-ol.*

Freshly prepared THP-protected 3-Butynol (2.5 g, 16.23 mmol) was added dropwise to a suspension of NaNH<sub>2</sub> (1.54 g of a 50% suspension in toluene, 19.5 mmol) in THF (15 ml) at 0°C. After 1h, DMSO (15 ml) and 1-Bromohexadecane (5.4 g, 17.7mmol) were added and the mixture was stirred for 3h at room temperature. The reaction mixture was quenched with water (20 ml) and extracted with diethylether (3  $\times$  25 ml). The combined organic phases were washed with brine and dried over MgSO<sub>4</sub>. After filtration, the solvent was removed via rotavap and the residue was chromatographed on silica gel (20:1 to 15:1 hexane/EtOAc) to obtain 1-[Tetrahydropyranyl]oxy]-3-eicosyne, which was immediately dissolved in 30 mL MeOH and treated with 20 mg *p*-Toluenesulfonic acid. After 1h at room temperature, 20 mL of saturated NaHCO<sub>3</sub>-solution were added and the mixture was extracted with diethylether (3  $\times$  25ml). The combined organic phases were washed with water (25 ml) and brine (15 ml) and dried over MgSO<sub>4</sub>. After filtration, the solvent was removed via rotavap and the residue was chromatographed on silica gel (9:1 hexane/EtOAc) to obtain 3-Eicosyn-1-ol (2.1 g, 44% yield over two steps). <sup>1</sup>H-NMR: (400 MHz, CDCl<sub>3</sub>)  $\delta$  = 3.67 (t,  $J$  = 6.3 Hz, 2H), 2.41 (tt, <sup>3</sup> $J$  = 9.3 Hz, <sup>5</sup> $J$  = 2.4 Hz, 2H), 2.14 (tt, <sup>3</sup> $J$  = 10.6 Hz, <sup>5</sup> $J$  = 2.4 Hz, 2H), 1.48 (m, 2H), 1.30 (m, 26H), 0.89 (t,  $J$  = 6.8 Hz, 3H)ppm; <sup>13</sup>C-NMR: (100 MHz, CDCl<sub>3</sub>)  $\delta$  = 82.5, 76.3, 61.3, 31.9, 29.7, 29.6, 29.5, 29.4, 29.3, 29.2, 29.1, 29.0, 28.9, 23.1, 22.6, 18.7, 14.0 ppm.

##### *Synthesis of 19-Eicosyn-1-ol.*

Ethylene-1,2-diamine (11 ml) was cooled to 0°C and 1.02 g NaH (60% in mineral oil, 25.5 mmol) were added. The mixture was allowed to warm to room temperature and stirred for 2 h. The violet mixture was heated to 60°C and stirred for 1h, before it was cooled to 40°C. At this temperature 3-eicosyn-1-ol (1.2 g, 4 mmol) was added. The green reaction mixture was then heated to 70°C and stirred for 5 h. After cooling to 0°C HCl<sub>aq</sub> (0.5 M, 20 ml) was added very carefully. The mixture was poured into a separatory funnel and HCl<sub>aq</sub> (1 M, 20ml) was added before extracting with diethylether (3  $\times$  20 ml). The combined organic phases were washed with HCl<sub>aq</sub> (1 M, 30ml) and brine (30 ml), dried over Na<sub>2</sub>SO<sub>4</sub> and concentrated under vacuum. Purification was done via column chromatography on silica gel (9:1 *n*-hexane/EtOAc) and 19-Eicosyn-1-ol (780 mg, 65%) was obtained as a white waxy solid. <sup>1</sup>H-NMR: (400 MHz, CDCl<sub>3</sub>)  $\delta$  = 3.64 (t,  $J$  = 6.6 Hz, 2H), 2.17 (td, <sup>3</sup> $J$  = 10.3 Hz, <sup>4</sup> $J$  = 2.6 Hz, 2H), 1.94 (t,  $J$  = 2.7 Hz, 1H), 1.54 (m, 4H), 1.30 (m, 28H) ppm; <sup>13</sup>C-NMR: (100 MHz, CDCl<sub>3</sub>)  $\delta$  = 84.8, 68.0, 63.1, 32.8, 29.7, 29.6, 29.5, 29.4, 29.3, 29.1, 28.8, 28.5, 25.7, 18.4 ppm.

##### *Synthesis of 19,22-Octacosadiyn-1-ol.*

To a suspension of CuI (1.01g, 5.3 mmol), NaI (800 mg, 5.3 mmol) and K<sub>2</sub>CO<sub>3</sub> (554 mg, 4 mmol) in DMF (10 ml), 1-bromo-2-octyn (550 mg, 2.91 mmol) and 19-Eicosyn-1-ol (780 mg, 2.65 mmol) were added. The suspension was stirred overnight and filtered over Celite®. The filtrate was poured into 20 mL of sat. NH<sub>4</sub>Cl and extracted with diethylether (3  $\times$  30 ml). The combined organic phases were washed with brine (30 ml), dried over Na<sub>2</sub>SO<sub>4</sub> and concentrated under vacuum. Purification was done via column chromatography on silica gel (12:1 *n*-hexane/EtOAc) and 19,22-Octacosadiyn-1-ol (737 mg,

69%) was obtained as a white waxy solid. <sup>1</sup>H-NMR: (400 MHz, CDCl<sub>3</sub>) δ = 3.63 (t, *J* = 6.5 Hz, 2H), 3.12 (quin, <sup>5</sup>*J* = 2.4 Hz, 2H), 2.14 (tt, <sup>3</sup>*J* = 10.5 Hz, <sup>5</sup>*J* = 2.3 Hz, 4H), 1.52 (m, 6H), 1.30 (m, 32H), 0.90 (t, *J* = 6.4 Hz, 3H) ppm; <sup>13</sup>C-NMR: (100 MHz, CDCl<sub>3</sub>) δ = 80.5, 74.5, 63.0, 32.8, 31.1, 29.7, 29.6, 29.5, 29.4, 29.3, 29.1, 29.0, 28.9, 28.8, 28.5, 25.7, 22.2, 18.72, 18.70, 13.9, 9.7 ppm.

*Synthesis of 19,22-Octacosadiynyl acetate.*

19,22-Octacosadiyn-1-ol (435 mg, 1.08 mmol) were dissolved in 10 mL dichloromethane. Acetic anhydride (234 μL, 2.2 mmol), triethylamine (345 μL, 2.2 mmol) and a few crystals of 4-dimethylaminopyridine were added and the solution stirred for 2 h. Water (10 ml) was added and the mixture was extracted with diethylether (3 × 15 ml). The combined organic phases were washed with brine (30 ml), dried over Na<sub>2</sub>SO<sub>4</sub> and concentrated under vacuum. Purification was done via column chromatography on silica gel (25:1 *n*-hexane/EtOAc) and 19,22-Octacosadiynyl acetate (435 mg, 90%) was obtained as a white waxy solid. <sup>1</sup>H-NMR: (400 MHz, CDCl<sub>3</sub>) δ = 4.05 (t, *J* = 6.8 Hz, 2H), 3.11 (quin, <sup>5</sup>*J* = 2.4 Hz, 2H), 2.14 (tt, <sup>3</sup>*J* = 10.7 Hz, <sup>5</sup>*J* = 2.3 Hz, 4H), 2.04 (s, 3H), 1.61 (quin, *J* = 7.0 Hz, 2H), 1.48 (m, 4H), 1.30 (m, 32H), 0.89 (t, *J* = 6.7 Hz, 3H) ppm; <sup>13</sup>C-NMR: (100 MHz, CDCl<sub>3</sub>) δ = 171.2, 80.4, 74.5, 64.6, 31.1, 29.7, 29.6, 29.5, 29.4, 29.3, 29.1, 28.9, 28.8, 28.6, 28.5, 25.9, 22.2, 21.0, 18.72, 18.70, 13.9, 9.7 ppm.

*Synthesis of (19Z,22Z)-Octacosadienyl acetate.*

19,22-Octacosadiyn-1-ol acetate (200 mg, 0.44 mmol) was dissolved in 4 mL MeOH and hydrogenated in an H<sub>2</sub>-atmosphere in the presence of 15 mg Lindlar catalyst (Sigma). The reaction was monitored via GC-MS and after completion (ca. 15 h) the mixture was diluted with diethylether (15 ml), filtered over Celite® and concentrated in vacuum. Purification was done via reversed-phase column chromatography on C18-silica gel (3:1 MeOH/CHCl<sub>3</sub>) to obtain 19Z,22Z-Octacosadienyl acetate (180 mg, 91%) as a white waxy solid. <sup>1</sup>H-NMR: (400 MHz, CDCl<sub>3</sub>) δ = 5.35 (m, 4H), 4.05 (t, *J* = 6.8 Hz, 2H), 2.77 (t, *J* = 6.4 Hz, 2H), 2.05 (q, *J* = 6.8 Hz, 4H), 2.04 (s, 3H), 1.61 (quin, *J* = 7.0 Hz, 2H), 1.30 (m, 32H), 0.89 (t, *J* = 6.8 Hz, 3H) ppm; <sup>13</sup>C-NMR: (100 MHz, CDCl<sub>3</sub>) δ = 171.2, 130.2, 128.0, 64.7, 31.5, 29.7, 29.6, 29.5, 29.4, 29.3, 29.2, 28.6, 27.25, 27.20, 25.9, 25.6, 22.6, 21.0, 14.1 ppm; EI-MS [*m/z* (relative intensity)]: 54 (25), 55 (100), 56 (22), 57 (41), 61 (22), 67 (50), 68 (41), 69 (78), 70 (17), 71 (18), 80 (13), 81 (53), 82 (80), 83 (71), 84 (10), 85 (10), 95 (50), 96 (78), 97 (52), 109 (31), 110 (34), 111 (22), 123 (20), 124 (21), 137 (13), 138 (14), 152 (12), 390 (37), 391 (11), 448 (17 [M]<sup>+</sup>).

## REFERENCES AND NOTES

1. M. G. Ritchie, Sexual selection and speciation. *Annu. Rev. Ecol. Evol. Syst.* **38**, 79–102 (2007).
2. O. Seehausen, Y. Terai, I. S. Magalhaes, K. L. Carleton, H. D. J. Mrosso, R. Miyagi, I. van der Sluijs, M. V. Schneider, M. E. Maan, H. Tachida, H. Imai, N. Okada, Speciation through sensory drive in cichlid fish. *Nature* **455**, 620–626 (2008).
3. C. Smadja, R. K. Butlin, On the scent of speciation: The chemosensory system and its role in premating isolation. *Heredity* **102**, 77–97 (2009).
4. H. T. Spieth, Courtship behavior in *Drosophila*. *Annu. Rev. Entomol.* **19**, 385–405 (1974).
5. D. S. Manoli, M. Foss, A. Villella, B. J. Taylor, J. C. Hall, B. S. Baker, Male-specific *fruitless* specifies the neural substrates of *Drosophila* courtship behaviour. *Nature* **436**, 395–400 (2005).
6. Y. Ding, A. Berrocal, T. Morita, K. D. Longden, D. L. Stern, Natural courtship song variation caused by an intronic retroelement in an ion channel gene. *Nature* **536**, 329–332 (2016).
7. O. M. Ahmed, A. Avila-Herrera, K. M. Tun, P. H. Serpa, J. Peng, S. Parthasarathy, J.-M. Knapp, D. L. Stern, G. W. Davis, K. S. Pollard, N. M. Shah, Evolution of mechanisms that control mating in *Drosophila* males. *Cell Rep.* **27**, 2527–2536.e4 (2019).
8. L. F. Seeholzer, M. Seppo, D. L. Stern, V. Ruta, Evolution of a central neural circuit underlies *Drosophila* mate preferences. *Nature* **559**, 564–569 (2018).
9. M. R. E. Symonds, B. Wertheim, The mode of evolution of aggregation pheromones in *Drosophila* species. *J Evol. Biol.* **18**, 1253–1263 (2005).
10. T. O. Auer, R. Benton, Sexual circuitry in *Drosophila*. *Curr. Opin. Neurobiol.* **38**, 18–26 (2016).
11. S. Guo, J. Kim, Molecular evolution of *Drosophila* odorant receptor genes. *Mol. Biol. Evol.* **24**, 1198–1207 (2007).

12. A. Kurtovic, A. Widmer, B. J. Dickson, A single class of olfactory neurons mediates behavioural responses to a *Drosophila* sex pheromone. *Nature* **446**, 542–546 (2007).
13. H. K. M. Dweck, S. A. M. Ebrahim, M. Thoma, A. A. M. Mohamed, I. W. Keeseey, F. Trona, S. Lavista-Llanos, A. Svatoš, S. Sachse, M. Knaden, B. S. Hansson, Pheromones mediating copulation and attraction in *Drosophila*. *Proc. Natl. Acad. Sci. U.S.A.* **112**, E2829-E2835 (2015).
14. W. Liu, X. Liang, J. Gong, Z. Yang, Y.-H. Zhang, J.-X. Zhang, Y. Rao, Social regulation of aggression by pheromonal activation of Or65a olfactory neurons in *Drosophila*. *Nat. Neurosci.* **14**, 896-902 (2011).
15. A. Ejima, B. P. C. Smith, C. Lucas, W. van der Goes van Naters, C. J. Miller, J. R. Carlson, J. D. Levine, L. C. Griffith, Generalization of courtship learning in *Drosophila* is mediated by *cis*-vaccenyl acetate. *Curr. Biol.* **17**, 599–605 (2007).
16. V. Grabe, A. Strutz, A. Baschwitz, B. S. Hansson, S. Sachse, Digital in vivo 3D atlas of the antennal lobe of *Drosophila melanogaster*. *J. Comp. Neurol.* **523**, 530–544 (2015).
17. A. Couto, M. Alenius, B. J. Dickson, Molecular, anatomical, and functional organization of the *Drosophila* olfactory system. *Curr. Biol.* **15**, 1535–1547 (2005).
18. L. M. Matzkin, Ecological genomics of host shifts in *Drosophila mojavensis*. *Adv. Exp. Med. Biol.* **781**, 233–247 (2014).
19. W. J. Etges, Evolutionary genomics of host plant adaptation: Insights from *Drosophila*. *Curr. Opin. Insect Sci.* **36**, 96–102 (2019).
20. E. Pfeiler, S. Castrezana, L. K. Reed, T. A. Markow, Genetic, ecological and morphological differences among populations of the cactophilic *Drosophila mojavensis* from southwestern USA and northwestern Mexico, with descriptions of two new subspecies. *J. Nat. Hist.* **43**, 923–938 (2009).
21. A. Ruiz, W. B. Heed, M. Wasserman, Evolution of the *mojavensis* cluster of cactophilic *Drosophila* with descriptions of two new species. *J. Hered.* **81**, 30–42 (1990).

22. C. W. Allan, L. M. Matzkin, Genomic analysis of the four ecologically distinct cactus host populations of *Drosophila mojavensis*. *BMC Genomics* **20**, 732 (2019).
23. A. Crowley-Gall, P. Date, C. Han, N. Rhodes, P. Andolfatto, J. E. Layne, S. M. Rollmann, Population differences in olfaction accompany host shift in *Drosophila mojavensis*. *Proc. Biol. Sci.* **283**, 20161562 (2016).
24. B. D. Newby, W. J. Etges, Host preference among populations of *Drosophila mojavensis* (Diptera: Drosophilidae) that use different host cacti. *J. Insect Behav.* **11**, 691–712 (1998).
25. L. L. Knowles, T. A. Markow, Sexually antagonistic coevolution of a postmating-prezygotic reproductive character in desert *Drosophila*. *Proc. Natl. Acad. Sci. U.S.A.* **98**, 8692–8696 (2001).
26. T. A. Markow, Sexual isolation among populations of *Drosophila mojavensis*. *Evolution* **45**, 1525–1529 (1991).
27. W. J. Etges, M. A. Ahrens, Premating isolation is determined by larval-rearing substrates in Cactophilic *Drosophila mojavensis*. V. Deep geographic variation in epicuticular hydrocarbons among isolated populations. *Am. Nat.* **158**, 585–598 (2001).
28. S. Zawistowski, R. C. Richmond, Inhibition of courtship and mating of *Drosophila melanogaster* by the male-produced lipid, *cis*-vaccenyl acetate. *J. Insect Physiol.* **32**, 189–192 (1986).
29. J. Y. Yew, K. Dreisewerd, H. Luftmann, J. Müthing, G. Pohlentz, E. A. Kravitz, A new male sex pheromone and novel cuticular cues for chemical communication in *Drosophila*. *Curr. Biol.* **19**, 1245–1254 (2009).
30. W. van der Goes van Naters, J. R. Carlson, Receptors and neurons for fly odors in *Drosophila*. *Curr. Biol.* **17**, 606–612 (2007).
31. L. L. Prieto-Godino, R. Rytz, S. Cruchet, B. Bargeton, L. Abuin, A. F. Silbering, V. Ruta, M. Dal Peraro, R. Benton, Evolution of acid-sensing olfactory circuits in drosophilids. *Neuron* **93**, 661–676.e6 (2017).

32. T. O. Auer, M. A. Khallaf, A. F. Silbering, G. Zappia, K. Ellis, R. Álvarez-Ocaña, J. R. Arguello, B. S. Hansson, G. S. X. E. Jefferis, S. J. C. Caron, M. Knaden, R. Benton, Olfactory receptor and circuit evolution promote host specialization. *Nature* **579**, 402–408 (2020).
33. V. Grabe, A. Baschwitz, H. K. M. Dweck, S. Lavista-Llanos, B. S. Hansson, S. Sachse, Elucidating the neuronal architecture of olfactory glomeruli in the *Drosophila* antennal lobe. *Cell Rep.* **16**, 3401–3413 (2016).
34. W. J. Etges, K. F. Over, C. C. De Oliveira, M. G. Ritchie, Inheritance of courtship song variation among geographically isolated populations of *Drosophila mojavensis*. *Anim. Behav.* **71**, 1205–1214 (2006).
35. J. S. R. Chin, S. R. Ellis, H. T. Pham, S. J. Blanksby, K. Mori, Q. L. Koh, W. J. Etges, J. Y. Yew, Sex-specific triacylglycerides are widely conserved in *Drosophila* and mediate mating behavior. *eLife* **3**, e01751 (2014).
36. J. Kohl, P. Huoviala, G. S. X. E. Jefferis, Pheromone processing in *Drosophila*. *Curr. Opin. Neurobiol.* **34**, 149–157 (2015).
37. V. Ruta, S. R. Datta, M. L. Vasconcelos, J. Freeland, L. L. Looger, R. Axel, A dimorphic pheromone circuit in *Drosophila* from sensory input to descending output. *Nature* **468**, 686–690 (2010).
38. P. M. O'Grady, T. A. Markow, Rapid morphological, behavioral, and ecological evolution in *Drosophila*: Comparisons between the endemic Hawaiian *Drosophila* and the cactophilic repleta species group. *Rapidly Evolving Genes and Genetic Systems* **1**, 176–186 (2012).
39. D. Mercier, Y. Tsuchimoto, K. Ohta, H. Kazama, Olfactory landmark-based communication in interacting *Drosophila*. *Curr. Biol.* **28**, 2624–2631.e5 (2018).
40. S. Lebreton, V. Grabe, A. B. Omondi, R. Ignell, P. G. Becher, B. S. Hansson, S. Sachse, P. Witzgall, Love makes smell blind: Mating suppresses pheromone attraction in *Drosophila* females via Or65a olfactory neurons. *Sci. Rep.* **4**, 7119 (2014).

41. I. W. Keeseey, V. Grabe, L. Gruber, S. Koerte, G. F. Obiero, G. Bolton, M. A. Khallaf, G. Kunert, S. Lavista-Llanos, D. R. Valenzano, J. Rybak, B. A. Barrett, M. Knaden, B. S. Hansson, Inverse resource allocation between vision and olfaction across the genus *Drosophila*. *Nat. Commun.* **10**, 1162 (2019).
42. J. Stökl, A. Strutz, A. Dafni, A. Svatos, J. Doubsky, M. Knaden, S. Sachse, B. S. Hansson, M. C. Stensmyr, A deceptive pollination system targeting drosophilids through olfactory mimicry of yeast. *Curr. Biol.* **20**, 1846–1852 (2010).
43. F. Kaftan, V. Vrkoslav, P. Kynast, P. Kulkarni, S. Böcker, J. Cvačka, M. Knaden, A. Svatoš, Mass spectrometry imaging of surface lipids on intact *Drosophila melanogaster* flies. *J. Mass Spectrom.* **49**, 223–232 (2014).
44. P. Horká, V. Vrkoslav, R. Hanus, K. Pecková, J. Cvačka, New MALDI matrices based on lithium salts for the analysis of hydrocarbons and wax esters. *J. Mass Spectrom.* **49**, 628–638 (2014).
45. P. Date, H. K. M. Dweck, M. C. Stensmyr, J. Shann, B. S. Hansson, S. M. Rollmann, Divergence in olfactory host plant preference in *D. mojavensis* in response to cactus host use. *PLOS One* **8**, e70027 (2013).
46. S. B. Olsson, B. S. Hansson, Electroantennogram and single sensillum recording in insect antennae. *Methods Mol. Biol.* **1068**, 157–177 (2013).
47. S. J. Moon, M. Köttgen, Y. Jiao, H. Xu, C. Montell, A taste receptor required for the caffeine response in vivo. *Curr. Biol.* **16**, 1812–1817 (2006).
48. K. Katoh, D. M. Standley, MAFFT multiple sequence alignment software version 7: Improvements in performance and usability. *Mol. Biol. Evol.* **30**, 772–780 (2013).
49. D.-D. Zhang, C. Löfstedt, Functional evolution of a multigene family: Orthologous and paralogous pheromone receptor genes in the turnip moth, *Agrotis segetum*. *PLOS One* **8**, e77345 (2013).
50. F. Gonzalez, P. Witzgall, W. B. Walker III, Protocol for heterologous expression of insect odourant receptors in *Drosophila*. *Front. Ecol. Evol.* **4**, 24 (2016).

51. J. Bischof, R. K. Maeda, M. Hediger, F. Karch, K. Basler, An optimized transgenesis system for *Drosophila* using germ-line-specific  $\phi$ C31 integrases. *Proc. Natl. Acad. Sci. U.S.A.* **104**, 3312–3317 (2007).
52. E. K. Brinkman, T. Chen, M. Amendola, B. van Steensel, Easy quantitative assessment of genome editing by sequence trace decomposition. *Nucleic Acids Res.* **42**, e168 (2014).
53. T. Dekker, I. Ibba, K. P. Siju, M. C. Stensmyr, B. S. Hansson, Olfactory shifts parallel superspecialism for toxic fruit in *Drosophila melanogaster* sibling, *D. sechellia*. *Curr. Biol.* **16**, 101–109 (2006).
54. Y. Kondoh, K. Y. Kaneshiro, K. Kimura, D. Yamamoto, Evolution of sexual dimorphism in the olfactory brain of Hawaiian *Drosophila*. *Proc. Biol. Sci.* **270**, 1005–1013 (2003).
55. R. M. Waterhouse, M. Seppey, F. A. Simão, M. Manni, P. Ioannidis, G. Klioutchnikov, E. V. Kriventseva, E. M. Zdobnov, BUSCO applications from quality assessments to gene prediction and phylogenomics. *Mol. Biol. Evol.* **35**, 543–548 (2018).
56. R. C. Edgar, MUSCLE: Multiple sequence alignment with high accuracy and high throughput. *Nucleic Acids Res.* **32**, 1792–1797 (2004).
57. M. N. Price, P. S. Dehal, A. P. Arkin, FastTree 2 – Approximately maximum-likelihood trees for large alignments. *PLOS One* **5**, e9490 (2010).
58. N. Shimosako, D. Hadjieconomou, I. Salecker, Flybow to dissect circuit assembly in the *Drosophila* brain. *Methods Mol. Biol.* **1082**, 57–69 (2014).
59. T. A. Markow, Evolution of *Drosophila* mating systems. *Evol. Biol.* **29**, 73–106 (1996).
60. L. L. Prieto-Godino, A. F. Silbering, M. A. Khallaf, S. Cruchet, K. Bojkowska, S. Pradervand, B. S. Hansson, M. Knaden, R. Benton, Functional integration of “undead” neurons in the olfactory system. *Sci. Adv.* **6**, eaaz7238 (2020).